

# On 1-D traveltimes tomography and linear inhomogeneity

Md Abu Sayed\*

## Abstract

In this article, we develop a 1-D traveltimes tomography method to calculate the seismic  $P$ -wave velocity of a medium. We use the results of 1-D tomography to obtain linear inhomogeneity parameters in a specific layer. To get the trustworthiness of the method, we perform several synthetic experiments. We show that the inverted model parameters are reasonably accurate and stable. To examine the results of linear inhomogeneity parameters using a different method, we also develop an inversion method based on a two-parameter velocity model. Finally, we apply both the methods to Vertical Seismic Profile (VSP) data and do a study comparing their results.

## 1 Introduction

We examine linear inhomogeneity of a medium by applying two inversion methods on seismic traveltimes. In the first method, we derive an analytical expression for the solution of Hamilton's ray equation in vertically inhomogeneous and isotropic media. Considering the analytical solution as a forward model, we construct an inversion method based on the Levenberg-Marquardt damped least square solution (Levenberg (1944), Marquardt (1963)). In the second inversion method, we use the traveltimes expression based on a two-parameter velocity model as the forward model. We perform several synthetic experiments on the first method based on a linear velocity model. While we study the linear velocity in synthetic studies to reduce the model parameters to two, the inversion method can be used to construct a velocity model that varies with depth in any order.

The synthetic experiments show that the traveltimes convergence occurs even with a significant change in the start-up values; however, as the discrepancy gets higher, the inverted velocity diverges more from the reference velocity model. In comparison to the start-up values, the inversion method is less sensitive to the number of data points and the noise.

We provide the source codes in the appendices A.1, A.2, and A.3. The checkshot (VSP) data is provided by the Canada-Newfoundland & Labrador Offshore Petroleum Board (C-NLOPB, 2019). Therein, the traveltimes data corresponds to a single source and multiple receivers. The source is placed at a 26.50 m offset, and the receivers are located along the vertical axis, starting at a depth of 1865 m and ending at 2650 m.

## 2 Method development

### 2.1 Solution of the ray equation in vertically inhomogeneous media

In a medium, the velocity of seismic waves can vary in any direction. However, assuming the velocity only a function of vertical depth, we present an analytical solution for Hamilton's ray equation. In the derivation, we apply the method of characteristics, similar to the approaches described by Slawinski (2015) and Červený (2001). To parameterize the ray equation, Slawinski (2015) used arc length as opposed to traveltimes, and Červený (2001) used the level set equation  $p^2 - v^{-2} = 0$  as opposed to

---

\*Department of Earth Sciences, Memorial University of Newfoundland, m.abusayed.stu@gmail.com

$p^2 v^2 = 1$ , where  $p$  is the slowness parameter, and  $v$  is the wave velocity. In our derivation, we use travelttime for the parametrization and  $p^2 v^2 = 1$  as the level set equation.

In this section, we present the solution of Hamilton's ray equation for a vertically inhomogeneous and isotropic medium. We start with a 3-D inhomogeneous medium and then move into a 1-D medium by considering velocity as a function of depth. In a smoothly inhomogeneous isotropic medium, the high-frequency seismic wave field can be separated into two independent waves,  $P$  and  $S$  (Slawinski, 2015, p. 277). Both waves satisfy the eikonal equation

$$p^2 = \frac{1}{v^2(\mathbf{x}, \mathbf{p})}, \quad (1)$$

where,  $p^2 = \mathbf{p} \cdot \mathbf{p}$ ,  $\mathbf{p}$  is the slowness and  $p_i := \frac{\partial \psi}{\partial x_i}$ ,  $i \in \{1, 2, 3\}$ ,  $\psi$  is the phase function. Equation (1) is a set of first order partial differential equations that depends on the variables  $\mathbf{x}$  and  $\mathbf{p}(\mathbf{x})$ . It relates the magnitude of phase slowness of the wave to the medium properties (Slawinski, 2015). The method of characteristics is commonly applied in the eikonal equation to get a system of six first-order ordinary differential equations (Slawinski, 2015, p. 343)

$$\begin{aligned} \frac{dx_i}{ds} &= \zeta \frac{\partial F}{\partial p_i}, \\ \frac{dp_i}{ds} &= -\zeta \frac{\partial F}{\partial x_i}, \end{aligned} \quad i \in \{1, 2, 3\}, \quad (2)$$

where  $\zeta$  is a scaling factor and  $s$  is the parameter along the curve. The choice of  $s$  determines the parametrization. As discussed in Slawinski (2015, p. 343), the solution of the eikonal equation is a surface in the  $\mathbf{x}\mathbf{p}$ -space. This surface can be described as level sets of a function, which we denote by  $F(\mathbf{x}, \mathbf{p})$ . It is a Hamiltonian with a factor of  $\frac{1}{2}$ . A relationship for the scaling factor  $\zeta$  in equation (2) to the flow parameter  $s$  are provided in Červený (2001). They consider three cases of  $s$  along the curve: the arclength, the travelttime and the parameter  $\sigma$ .

For a vertically inhomogeneous isotropic medium, we solve Hamilton's ray equation by parametrizing the characteristic equations in terms of time and scaling factor as a constant number, so that expression (2) becomes

$$\begin{aligned} \dot{x}_i &= \frac{\partial}{\partial p_i} \left( \frac{F}{2} \right) = \frac{\partial \mathcal{H}}{\partial p_i}, \\ \dot{p}_i &= -\frac{\partial}{\partial x_i} \left( \frac{F}{2} \right) = -\frac{\partial \mathcal{H}}{\partial x_i}, \end{aligned} \quad i \in \{1, 2, 3\}, \quad (3)$$

where  $\mathcal{H} := \frac{F}{2}$ , known as the ray-theory Hamiltonian. We choose  $F(\mathbf{x}, \mathbf{p}) = p^2 v^2(\mathbf{x}, \mathbf{p})$  as the level sets, which leads to a Hamiltonian

$$\mathcal{H}(\mathbf{x}, \mathbf{p}) = \frac{1}{2} p^2 v^2(\mathbf{x}) = \frac{1}{2} [p_1, p_3] \cdot [p_1, p_3] v^2(x_1, x_3), \quad (4)$$

and the corresponding ray equations

$$\frac{dx_1}{dt} = p_1 v^2, \quad (5a)$$

$$\frac{dx_3}{dt} = p_3 v^2, \quad (5b)$$

$$\frac{dp_1}{dt} = -p^2 v \frac{\partial v}{\partial x_1} = 0, \quad (5c)$$

$$\frac{dp_3}{dt} = -p^2 v \frac{\partial v}{\partial x_3}. \quad (5d)$$

Dividing expression (5a) by (5b)

$$\frac{dx_1}{dx_3} = \frac{p_1}{p_3}. \quad (6)$$

Using the eikonal equation  $p_1^2 + p_3^2 = v^{-2}$  in expression (6)

$$\frac{dx_1}{dx_3} = \frac{p_1}{\sqrt{v^{-2} - p_1^2}} = \frac{p_1 v}{\sqrt{1 - p_1^2 v^2}}. \quad (7)$$

Using expression (7) in expression (5a)

$$dt = \frac{dx_1}{p_1 v^2} = \frac{\frac{p_1 v}{\sqrt{1 - p_1^2 v^2}} dx_3}{p_1 v^2} = \frac{dx_3}{v \sqrt{1 - p_1^2 v^2}}. \quad (8)$$

Expression (5c) shows that the slowness parameter,  $p_1$ , is constant along the whole ray path. For a vertically inhomogeneous medium  $p_1$  is a conserved quantity, which is known as the ray parameter. We express the ray parameter by  $\mathbf{p}$ . We obtain the solution of ray equation by integrating expressions (6) and (8) for  $x_3$  to get

$$x_1(x_3) = \int_{z_0}^z \frac{\mathbf{p} v(x_3)}{\sqrt{1 - \mathbf{p}^2 v^2(x_3)}} dx_3, \quad (9)$$

and

$$t(x_3) = \int_{z_0}^z \frac{1}{v \sqrt{1 - \mathbf{p}^2 v^2(x_3)}} dx_3, \quad (10)$$

where  $x_3$  is the vertical depth. Equations (9) and (10) are in agreement with Červený (2001). To trace a ray, we need to solve expressions (9) and (10) simultaneously.

If the velocity changes linearly with depth, i.e.,  $v(x_3) = a + bx_3$ , using expressions (9) and (10), the ray parameter and the traveltimes expressions can be written as (Slawinski and Slawinski, 1999)

$$\mathbf{p} = \frac{2bx_3}{\sqrt{(b^2 x_3^2 + a^2 + (a + bx_3)^2) - 4a^2(a + bx_3)^2}}, \quad (11)$$

$$t = \frac{1}{b} \left| \log \left( \frac{a + bx_3}{a} \frac{1 + \sqrt{1 - a^2 \mathbf{p}^2}}{1 + \sqrt{1 - \mathbf{p}^2 (a + bx_3)^2}} \right) \right|. \quad (12)$$

We use expression (12) as the forward model to the  $ab$ -model inversion.

## 2.2 Discretizing the forward model for 1-D tomography

In this section, we discretize the expressions (9) and (10) to solve the ray equation numerically. To perform the integration for multiple source-receiver pairs, we consider the medium to be composed of  $N$  layers;  $H$  is the layer thickness, where the layers are equally thin, homogeneous, and isotropic. Using expressions (9) and (10), the ray tracing equations from the  $i$ -th source to the  $k$ -th receiver are

$$x_{k,i} = x_{1k,i} + x_{2k,i} + \dots + x_{jk,i} = \sum_{j=1}^m \frac{H_j B_{kj,i}}{\sqrt{1 - B_{kj,i}^2}}, \quad j \in \{1, 2, 3, \dots, m\}, \quad (13)$$

$$t_{k,i} = t_{1k,i} + t_{2k,i} + \dots + t_{jk,i} = \sum_{j=1}^m \frac{H_j}{v_j \sqrt{1 - B_{kj,i}^2}}, \quad j \in \{1, 2, 3, \dots, m\}, \quad (14)$$

where  $\theta_{1k}$  is the take-off angle,  $B_{kj,i} = p_{k,i}v_j$ ,  $i$  and  $k$  denote the indices of sources and receivers. Traveltime in the  $j$ -th segment is  $t_{jk}$ . The total number of model parameters is  $m$ , which is equal to the number of layers. We consider the sources to be located at the surface and the receivers to be set along the vertical axis. To calculate the total traveltime and the offset for a given source-receiver pair, we modify the upper limit of the summation by replacing  $m$  to  $L(k)$ . For a given source-receiver pair, we modify the upper limit of the summation by replacing  $m$  by  $L(k)$  to calculate the total traveltime and the offset. This is because, the Geophone locations may not be related to the layering, therefore, an index  $L(k)$  is introduced that indicates in which layer the  $k$ -th geophone is located. If the geophone locations  $k$  and  $k + 1$  are in the same layer, then  $L(k) = L(k + 1)$ .

### 2.3 Development of the inversion method for 1-D tomography

Using the analytical solution as a forward model, we develop an inversion method based on Levenberg-Marquardt (L-M) damped least-squares solution. The L-M method is a powerful tool for the iterative solution for both linear and nonlinear problems (Pujol, 2007). Levenberg (1944) used the technique for the first time, and about twenty years later, Marquardt (1963) independently rediscovered the method utilizing an independent approach.

In this section, we develop the L-M method for a vertically inhomogeneous and isotropic medium. As the forward model, we use expressions (13) and (14) from section 2.2. In the case of  $t = t(v_j)$ , the traveltime residual can be written as

$$dt_k = \sum_{j=1}^{L(k)} \frac{\partial t_k}{\partial v_j} dv_j, \quad j \in \{1, 2, 3, \dots, L(k)\}. \quad (15)$$

Where, we neglect the higher order terms in Taylor series expansion. Taking the derivative of expression (14) with respect to  $v_j$ ,

$$\frac{\partial t_k}{\partial v_j} = \frac{p_k^2 h_j}{\sqrt{1 - B_{kj}^2}} - \frac{h_j}{v_j^2 \sqrt{1 - B_{kj}^2}}, \quad j \in \{1, 2, 3, \dots, L(k)\}. \quad (16)$$

Also, the system of linear equations (15) may be written in the matrix form,

$$\mathbf{C} = \mathbf{t}_{\text{obs}} - \mathbf{t}_{\text{mod}} = \mathbf{A}\mathbf{X}, \quad (17)$$

where <sup>1</sup>

$$\mathbf{C} = (dt_1, dt_2, \dots, dt_M)^T \quad \text{and} \quad \mathbf{X} = (dv_1, dv_2, \dots, dt_N)^T. \quad (18)$$

In expression (17),  $\mathbf{A}$  is an  $(M \times N)$  matrix of partial derivatives,  $M$  and  $N$  are the total number of receivers and layers, respectively.  $\mathbf{X}$  represents the model parameter adjustment vector, and  $\mathbf{C}$  is the traveltime residual vector. We calculate both the traveltime residual vector and the partial derivative matrix in each iteration.

For a particular source-receiver pair, the basic algorithm is as follows—we apply the Newton-Raphson method to calculate the take-off angle from equation (13) by assuming we have the velocities in each layer. The corrected take-off angle is used to calculate the model traveltime. The parameter adjustment vector is calculated from expression (17), which allows us to update the velocity in each iteration. We repeat the process until we achieve a satisfactory agreement between the model and observed data.

To solve equation (17) for  $\mathbf{X}$ , Pujol (2007) stated that the convergence is not assured when  $\mathbf{X}$  is computed using ordinary least squares. The assumption behind linearizing the problem no longer remains valid if the initial model is far from the real solution. One of the ways to overcome this problem is the application of Levenberg-Marquardt method.

<sup>1</sup>Throughout the Chapter ??, we present vectors and matrices in bold letters.

## 2.4 A review of Levenberg-Marquardt Method

In this section, we review the basic steps of Levenberg-Marquardt iteration scheme. We follow the description of Pujol (2007). Let us consider the higher order terms in Taylor series expansion that we ignored in equation (17)

$$\mathbf{R} = \mathbf{C} - \mathbf{A}\mathbf{X}. \quad (19)$$

The elements of  $\mathbf{C}$  represent the residuals of travelttime for each source-receiver pair. The problem is to calculate the elements of  $\mathbf{X}$ 's which minimize  $\mathbf{R}$ . The misfit function is defined as follows,

$$S = \sum_{i=1}^n R_i^2 = \mathbf{R}^T \mathbf{R} \quad \{1, 2, 3, \dots, n\}, \quad (20)$$

where  $n$  is the number of data points. Substituting equation (19) into (20), we get

$$S = (\mathbf{C}^T - \mathbf{X}^T \mathbf{A}^T)(\mathbf{C} - \mathbf{A}\mathbf{X}) = \mathbf{C}^T \mathbf{C} - 2\mathbf{C}^T \mathbf{A}\mathbf{X} + \mathbf{X}^T \mathbf{A}^T \mathbf{A}\mathbf{X}. \quad (21)$$

Instead of minimizing the misfit function  $S$ , Levenberg (1944) proposes to minimize the following function

$$\bar{S} = wS + Q, \quad (22)$$

where  $w$  is known as Levenberg damping parameter,  $Q = \mathbf{X}^T \mathbf{D}\mathbf{X}$  with  $\mathbf{D} = \mathbf{I}$ , the identity matrix. Using equation (21) in equation (22)

$$\bar{S} = w \left( \mathbf{C}^T \mathbf{C} - 2\mathbf{C}^T \mathbf{A}\mathbf{X} + \mathbf{X}^T (\mathbf{A}^T \mathbf{A} + \frac{1}{w} \mathbf{I}) \mathbf{X} \right). \quad (23)$$

Minimizing Equation (23)

$$\frac{d\bar{S}}{d\mathbf{X}} = \left( \frac{d\bar{S}}{dX_1}, \frac{d\bar{S}}{dX_2}, \dots, \frac{d\bar{S}}{dX_N} \right)^T = \mathbf{0},$$

The iteration scheme becomes

$$(\mathbf{A}^T \mathbf{A} + \lambda \mathbf{I}) \mathbf{X} = \mathbf{A}^T \mathbf{c}, \quad (24)$$

where  $\lambda = \frac{1}{w}$ . Using the method of Pujol et al. (1985), we assign a constant value to  $\lambda$  and in each iteration we reduce it by a factor of 10. At  $p$ -th iteration, we solve

$$\left( (\mathbf{A}^T \mathbf{A})^{(p)} + \lambda^{(p)} \mathbf{I} \right) (\mathbf{X})^{(p)} = (\mathbf{A}^T \mathbf{c})^{(p)}. \quad (25)$$

To otherwise improve the numerical aspects of the method, we use the scaled version of equation (25), which is suggested by Marquardt (1963). Instead of using  $\mathbf{A}^T \mathbf{A}$  and  $\mathbf{A}^T \mathbf{c}$  in expression (25), we use the scaled forms  $[\mathbf{A}^T \mathbf{A}]^*$  and  $[\mathbf{A}^T \mathbf{c}]^*$ , The components of the scaled matrix are (Pujol, 2007)

$$\left( [\mathbf{A}^T \mathbf{A}]^* \right)_{ij} = S_{ii} S_{jj} (\mathbf{A}^T \mathbf{A})_{ij} \quad (26)$$

and

$$\left( [\mathbf{A}^T \mathbf{c}]^* \right)_i = S_{ii} (\mathbf{A}^T \mathbf{c})_i, \quad (27)$$

where

$$S_{ii} = \frac{1}{\sqrt{([\mathbf{A}^T \mathbf{A}]^*)_{ii}}}. \quad (28)$$

The scaled Levenberg-Marquardt equation is

$$\left( [\mathbf{A}^T \mathbf{A}]^{*(p)} + \lambda^{(p)} \mathbf{I} \right) \mathbf{X}^{*(p)} = [\mathbf{A}^T \mathbf{c}]^{*(p)}. \quad (29)$$

In each iteration step, we solve equation (29) for  $\mathbf{X}^*$  and then calculate the components of  $\mathbf{X}^*$  based on  $\mathbf{X}$ ,

$$X_i = S_{ii} X_i^*. \quad (30)$$

The vector form of expression (30) is

$$\mathbf{X} = \mathbf{S} \mathbf{X}^*, \quad (31)$$

where  $\mathbf{S}$  is a diagonal matrix with diagonal elements  $S_{ii}$ . In each iteration, we update the velocity as

$$\mathbf{V}^{(p+1)} = \mathbf{V}^{(p)} + \mathbf{X}^{(p)}. \quad (32)$$

The iteration process continues until we reach a specific value of the misfit functional. Under the assumption of uncorrelated data with equal variances,  $\sigma_0^2$ , at  $p$ -th iteration, the misfit functional is defined as (Zhdanov, 2002, p. 73)

$$f(\mathbf{X}^{(p)}) = \frac{1}{\sigma_0^2} \left( t_{obs} - t_{mod}^{(p)} \right)^2. \quad (33)$$

In synthetic cases, we add normally distributed noise to the traveltimes data, and following equation (33), we set the iteration to stop while  $f(\mathbf{X}^{(p)}) \approx N$ , where  $N$  is the number of data points.

In each iteration of the Levenberg-Marquardt method, for a given set of velocities in layers, we use equation (13) to update the take-off angle. We apply a root-finding algorithm known as the Newton-Raphson method (Heath, 2002) to calculate  $p_{k,i}$ . It produces successively better approximations to the roots of a real-valued function. To optimize the computation time, we terminate the iteration once we reach to the value of  $10^{-6}$  for the  $dx_1$ , which is the difference between the horizontal distance of the shooting ray and the offset given from the data.

The updated take-off angle is used to calculate the velocity in the next iteration of the Levenberg-Marquardt method. The process of calculation makes the method two-step as opposed to the one-step approach described by Pujol et al. (1985). The two-step approach provides us with a better initial model for the traveltimes since it calculates only the take-off angle in first and the velocity in the second. It also allows us to use a single unit for model parameters, which reduces the work of nondimensionalization to define misfit functional.

In contrast to the other local optimization method, such as Gauss-Newton or steepest descent method, the Levenberg-Marquardt method minimizes both model parameters and the data residuals (Pujol, 2007). As a result, the chances of convergence increases.

### 3 Synthetic experiments

In the synthetic experiments, we consider multiple sources at the surface, many receivers along the vertical depth and assign a reference velocity which changes linearly with depth. The linear velocity is described by two parameters, i.e., the velocity at the surface and the velocity gradient. The variations of both parameters in the startup model allow us to observe the influence of the initial model to the inversion result. We also study the effects of the noise on the data and the number of data points. In the synthetic study, the forward traveltimes is calculated based on the analytic solution, the observed traveltimes is calculated based on the variations in the reference velocity model by changing the startup model and the amount of noise in the data.

#### 3.1 Test of the noise and the number of data points

In Table 1, we consider the reference velocity model as a linear function of depth,  $v = a + bz$ , with  $a = 1000 \text{ ms}^{-1}$  and  $b = 0.12 \text{ s}^{-1}$ . We choose  $a$  based on the typical value of the  $P$ -wave velocity at the surface in the offshore. To have more options in choosing the number of layers in the synthetic experiments, we decide to consider the velocity gradient in the lower side, such as 0.12. If the velocity gradient is higher, with the increase of layers, the ray hits the critical angle in a relatively lower take-off

angle. For the first six cases, the startup velocity for inversion is considered as  $v_{ref} \pm 20 \text{ ms}^{-1}$  and for the last six cases, the startup velocity is considered as  $v_{ref} \pm 40 \text{ ms}^{-1}$ . Following Pujol et al. (1985), we choose the value of the parameter  $\lambda$  in the Levenberg-Marquardt algorithm. We start at  $10^4$ , and in each iteration, it reduces by a factor of 10. We consider the number of traveltimes data and the number of model parameters to be equal. However, the inversion method can be applied to both underdetermined and overdetermined cases.

Test	Noise (%)	Source	Geophone	Layer	$f(\mathbf{M})$	$a_{inv}$	$b_{inv}$	Figure
1	1	101	1	101	97.74	1002.15	0.1179	1a,2a
2	1	101	2	202	199.90	1001.46	0.1184	1b,2b
3	5	101	1	101	100.70	1002.17	0.1173	1c,2c
4	5	101	2	202	200.95	1001.73	0.1187	1d,2d
5	10	101	1	101	100.53	1002.40	0.1178	1e,2e
6	10	101	2	202	199.87	1002.22	0.1171	1f,2f
7	1	101	1	101	99.91	1003.42	0.1157	3a,4a
8	1	101	2	202	201.90	1003.15	0.1166	3b,4b
9	5	101	1	101	100.23	1002.62	0.1159	3c,4c
10	5	101	2	202	201.32	1001.91	0.1166	3d,4d
11	10	101	1	101	100.23	1004.20	0.1153	3e,4e
12	10	101	2	202	200.12	1002.48	0.1170	3f,4f

Table 1: Model set-up : test of the first six,  $a_{true} = 1000 \text{ ms}^{-1}$ ,  $b_{true} = 0.12 \text{ s}^{-1}$ ,  $a_{in} = a_{true} \pm 20 \text{ ms}^{-1}$ ,  $b_{in} = b_{true}$ ; test of the last six,  $a_{true} = 1000 \text{ ms}^{-1}$ ,  $b_{true} = 0.12 \text{ s}^{-1}$ ,  $a_{in} = a_{true} \pm 40 \text{ ms}^{-1}$ ,  $b_{in} = b_{true}$

In Table 1,  $f(\mathbf{M})$  provides the misfit functional,  $a_{inv}$  and  $b_{inv}$  present the model parameters after fitting a line to the inverted velocity. The traveltimes convergence results are shown in Figures 1 and 3. The misfits of the inverted velocity to the reference velocity are shown in Figures 2 and 4. To examine the effect of noise and the number of data points, we add 1%, 5% and 10% of random noises and 101 and 202 number of data points.

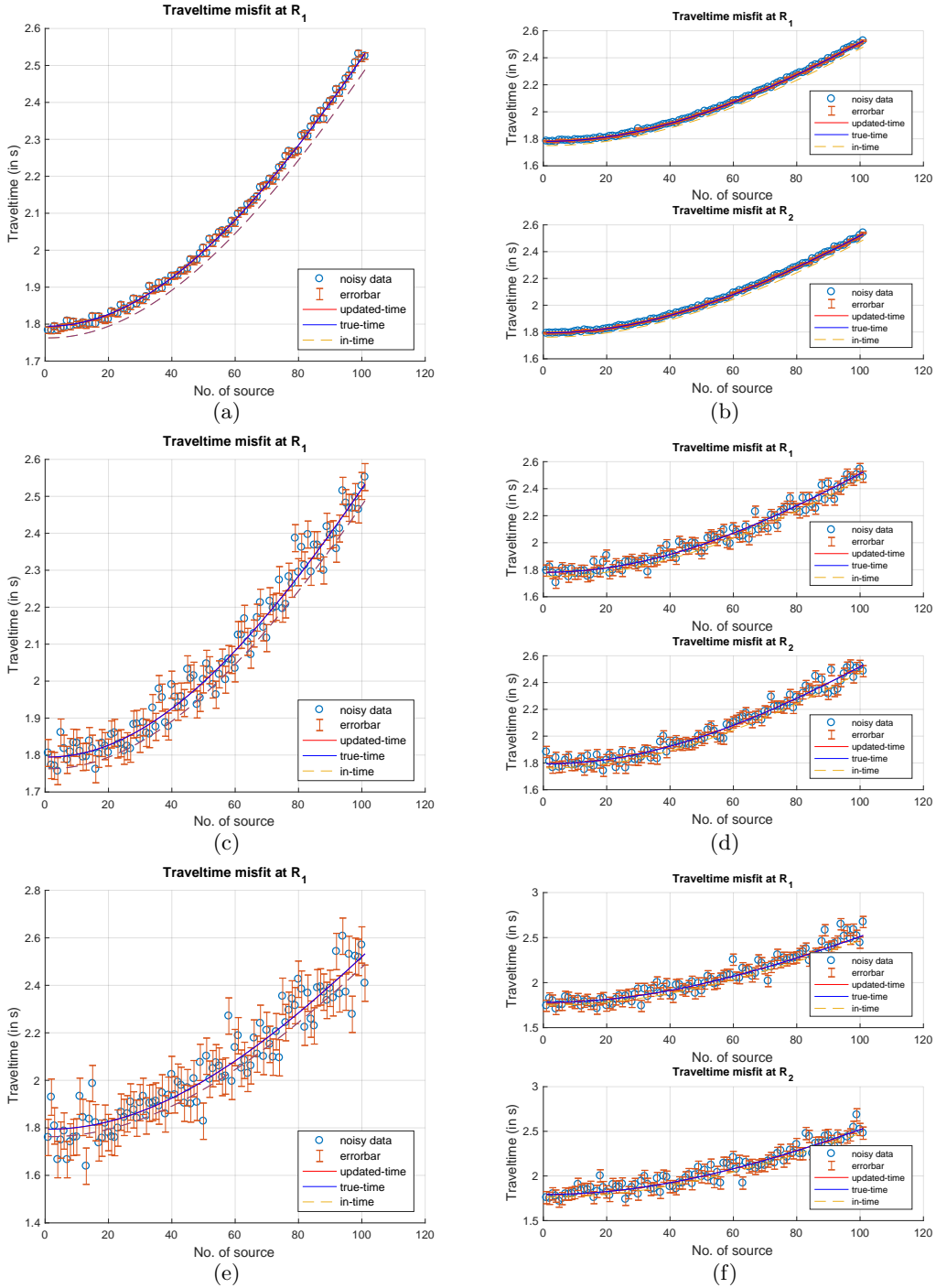


Figure 1: Travetime inversion: variation of noise and number of data points,  $v_{in} = v_{true} \pm 20$

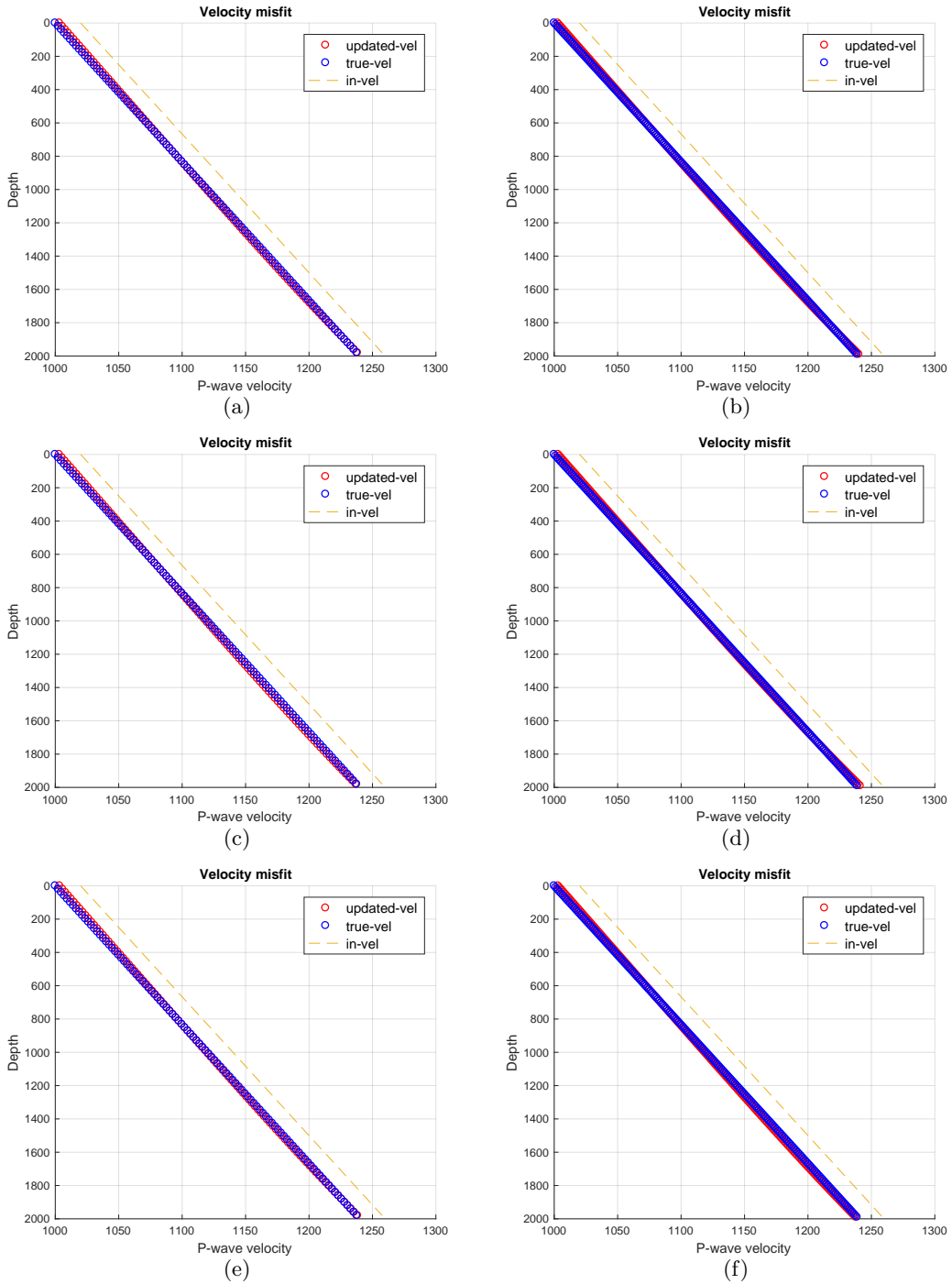


Figure 2: Velocity inversion : variation of noise and number of data points,  $v_{in} = v_{true} \pm 20$

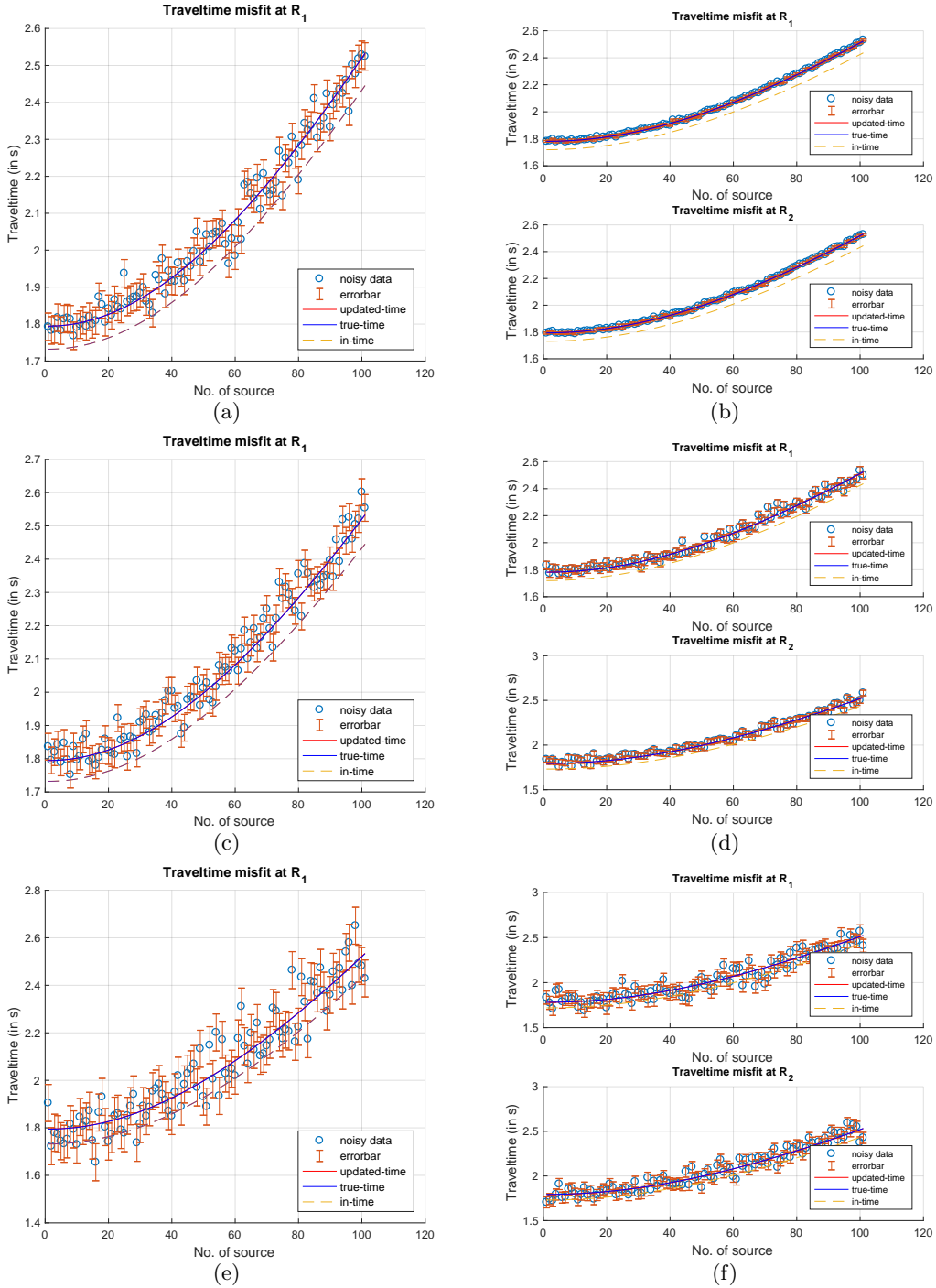


Figure 3: Travetime inversion: variation of noise and number of data points,  $v_{in} = v_{true} \pm 40$

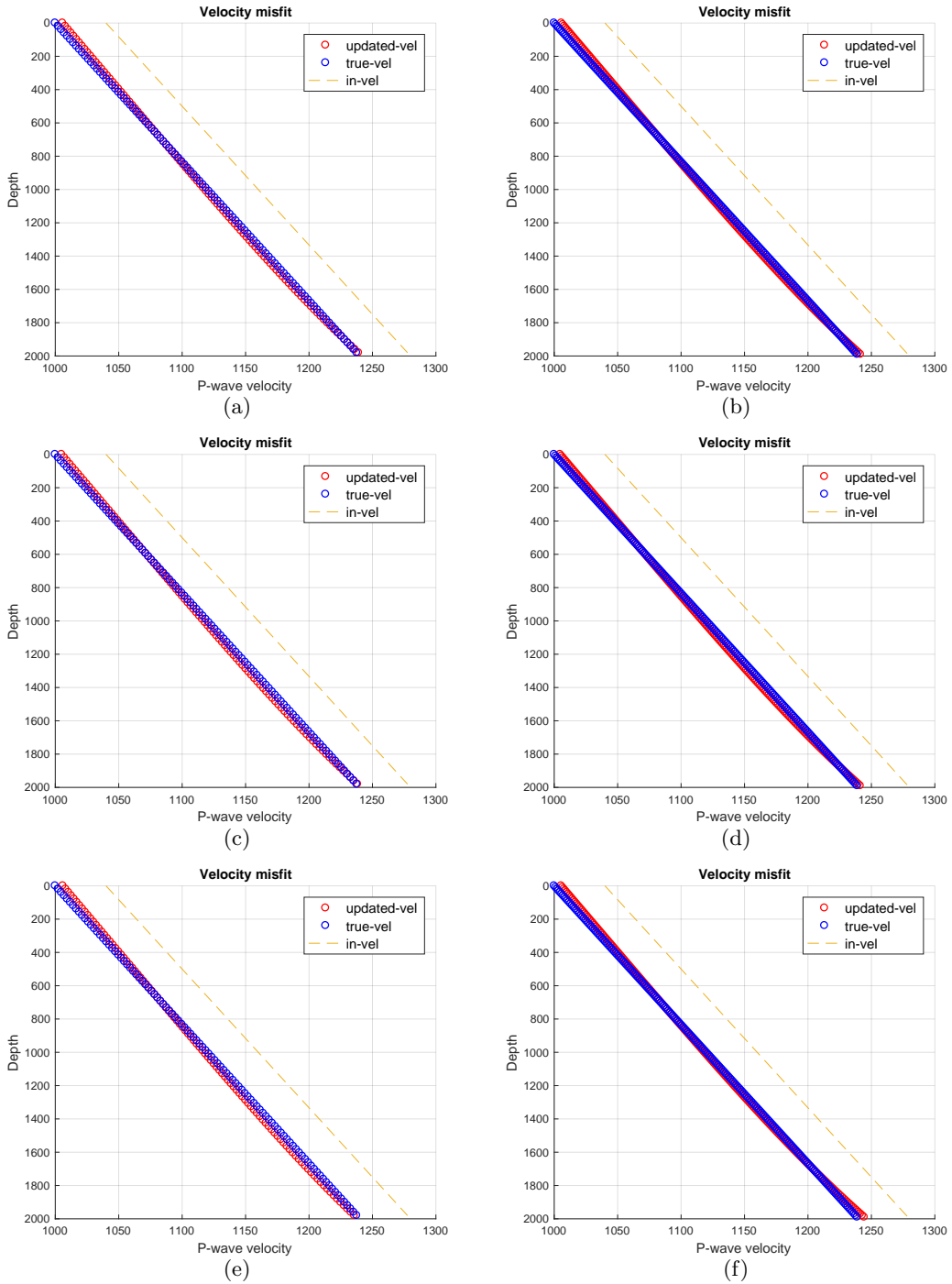


Figure 4: Velocity inversion : variation of noise and number of data points,  $v_{in} = v_{true} \pm 40$

### 3.2 Test of the model parameters $a$ and $b$

In Table 2, we consider the reference velocity model to be a linear function of depth, where parameters  $a = 1000 \text{ ms}^{-1}$  and  $b = 0.12 \text{ s}^{-1}$ . In contrast to Table 1, here we change the model parameter  $b$ . For the first six tests, the startup velocity for the inverse model is  $v_{ref} + \pm 30 \text{ ms}^{-1}$ , and for the last six tests, the startup velocity is  $v_{ref} \pm 60 \text{ ms}^{-1}$ . We set the noise to 1%, the number of data points to 202 and the total number of model parameters to 202.

The purpose of this section to show, for a given noise and data points, the effects of the startup model parameters  $a_{in}$  and  $b_{in}$  on the inversion. For  $b_{in}$ , we change it from  $b_{true} \rightarrow b_{true} \pm 0.01$ .

The traveltime convergence results are shown in Figures 5 and 7. The velocity misfits are shown in Figures 6 and 8.

Test	$a_{in}$	$b_{in}$	$a_{inv}$	$b_{inv}$	$f(\mathbf{M})$	Figure
1	970	0.1200	997.77	0.1225	201.07	5a,6a
2	970	0.1150	1002.05	0.1178	200.53	5b,6b
3	970	0.1100	1006.44	0.1130	201.56	5c,6c
4	1030	0.1200	1002.11	0.1178	199.09	5d,6d
5	1030	0.1250	998.19	0.1220	199.71	5e,6e
6	1030	0.1300	993.00	0.1275	198.04	5f,6f
7	940	0.1200	994.58	0.1257	201.30	7a,8a
8	940	0.1150	999.20	0.1209	196.79	7b,8b
9	940	0.1100	1003.75	0.1160	201.69	7c,8c
10	1060	0.1200	1005.02	0.1145	201.03	7d,8d
11	1060	0.1250	1000.29	0.1199	199.32	7e,8e
12	1060	0.1300	994.62	0.1259	198.07	7f,8f

Table 2: Model set-up: number of data points = 202, added noise up to 1%. test of the first six,  $a_{in} = a_{true} \pm 30$  and test of the last six,  $a_{in} = a_{true} \pm 60$  (units of  $a$  and  $b$  are  $\text{ms}^{-1}$  and  $\text{s}^{-1}$ )

Table 2 shows the inversion results to be more sensitive to the parameter  $b$  compared to the parameter  $a$ . However, the synthetic experiments show that the inversion method produces the reference velocity consistently within a small range of error. If we apply a good startup model and sufficient data points, the synthetic results show that the inversion method can produce a reasonable velocity model of a medium.

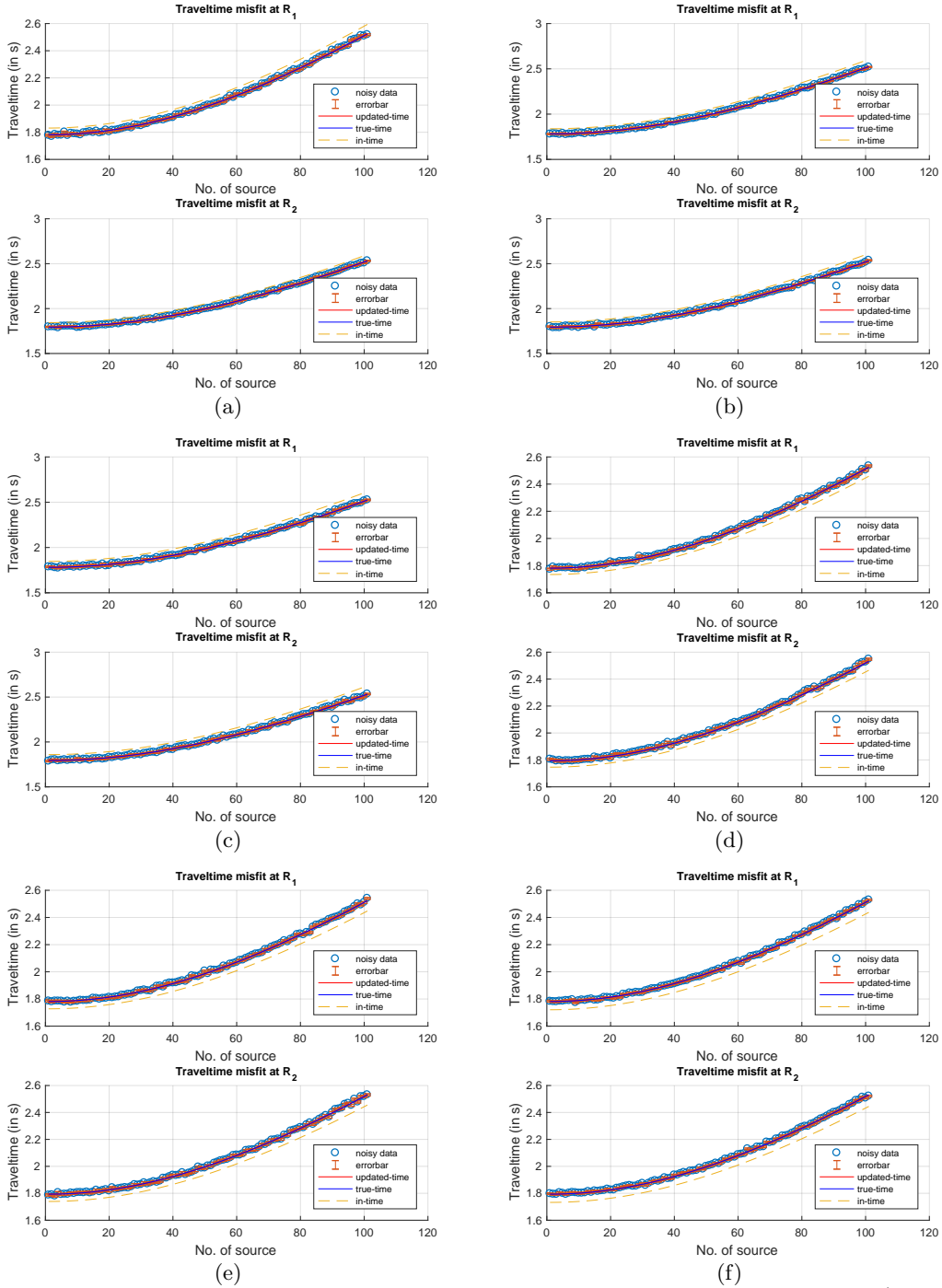


Figure 5: Traveltime inversion for different velocity gradients,  $v_{in} = v_{true} \pm 30 (ms^{-1})$ .

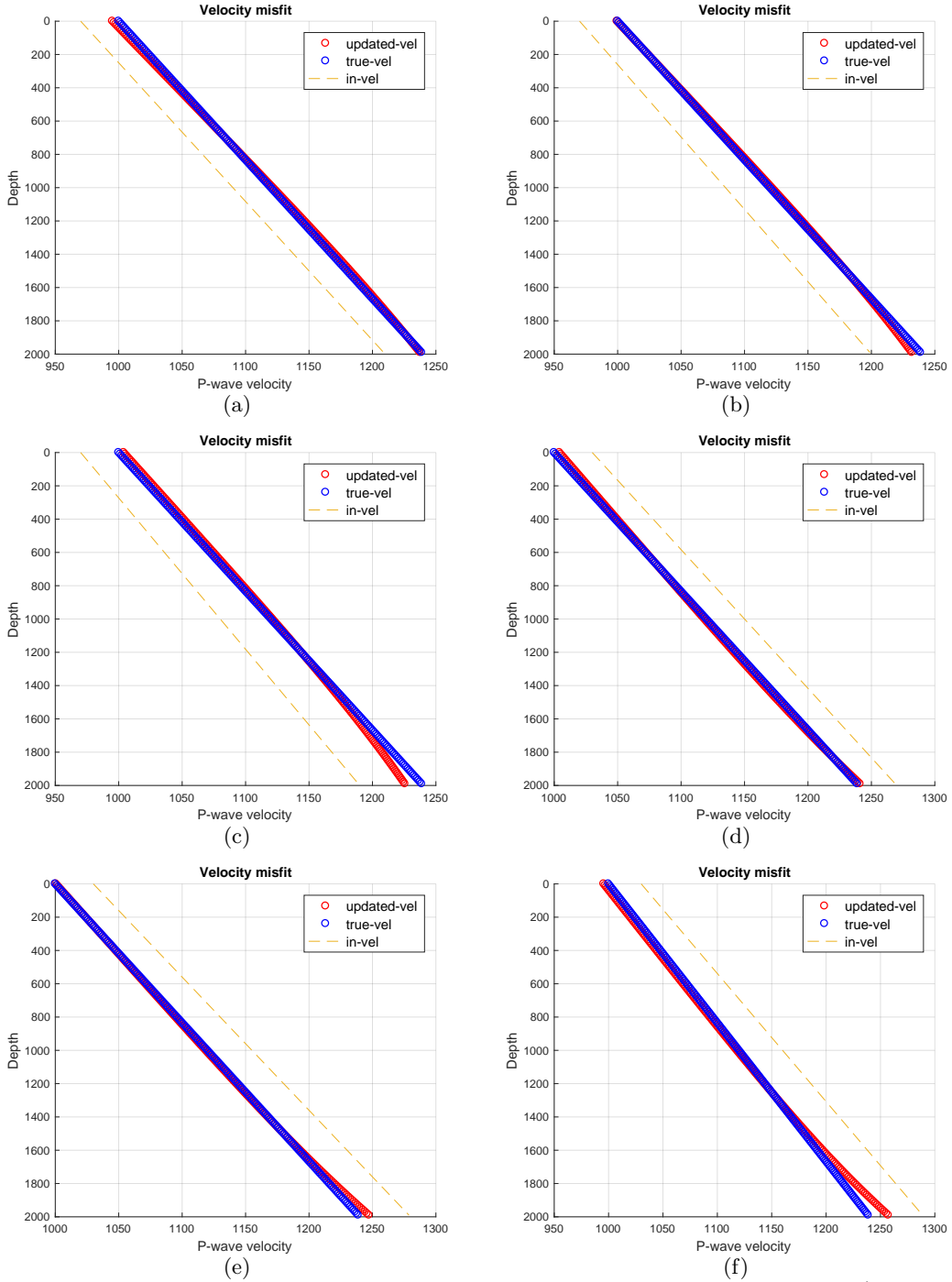


Figure 6: Velocity model for different velocity gradients,  $v_{in} = v_{true} \pm 30 (ms^{-1})$ .

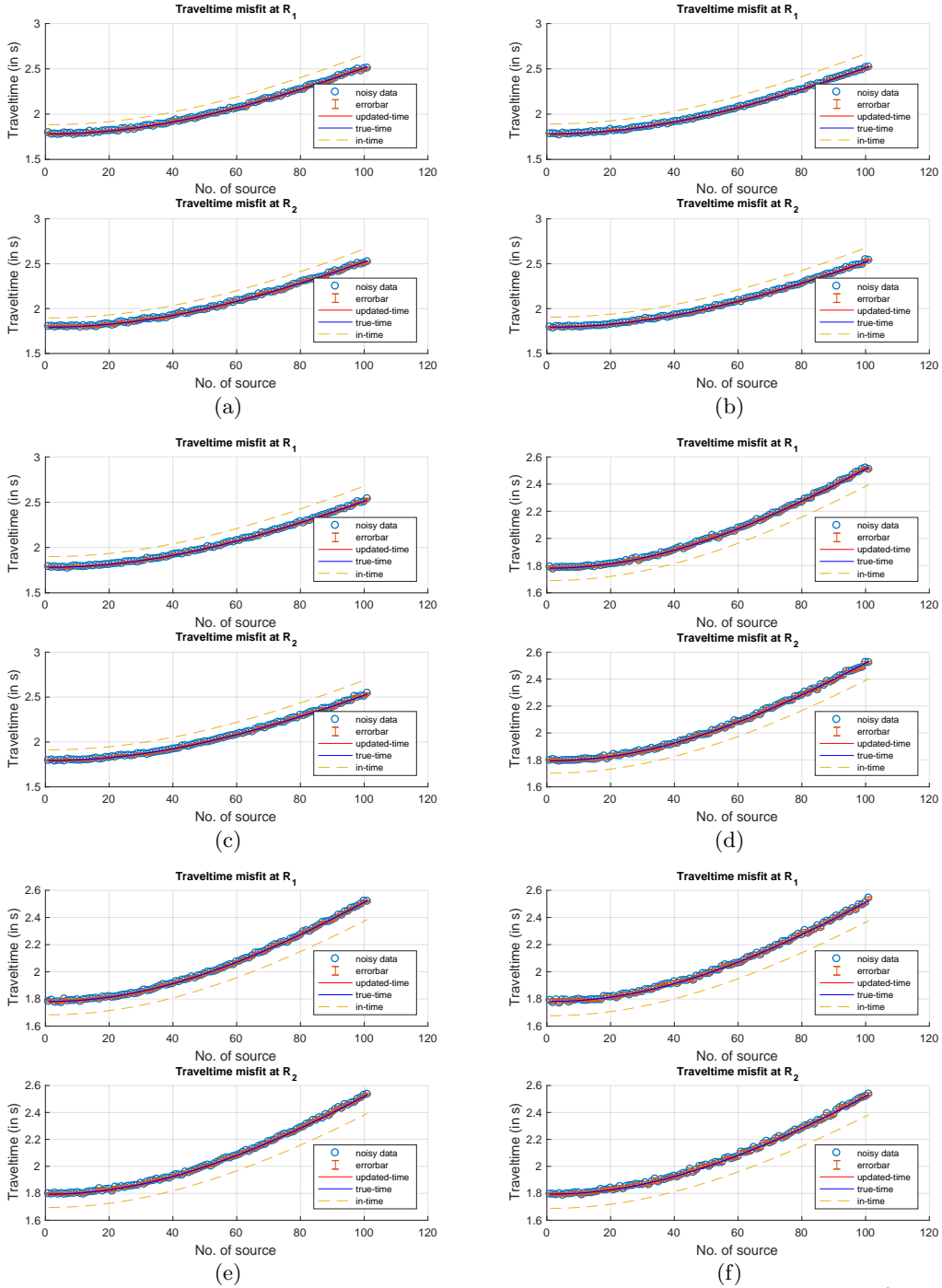


Figure 7: Traveltime inversion for different velocity gradients,  $v_{in} = v_{true} \pm 60 (ms^{-1})$ .

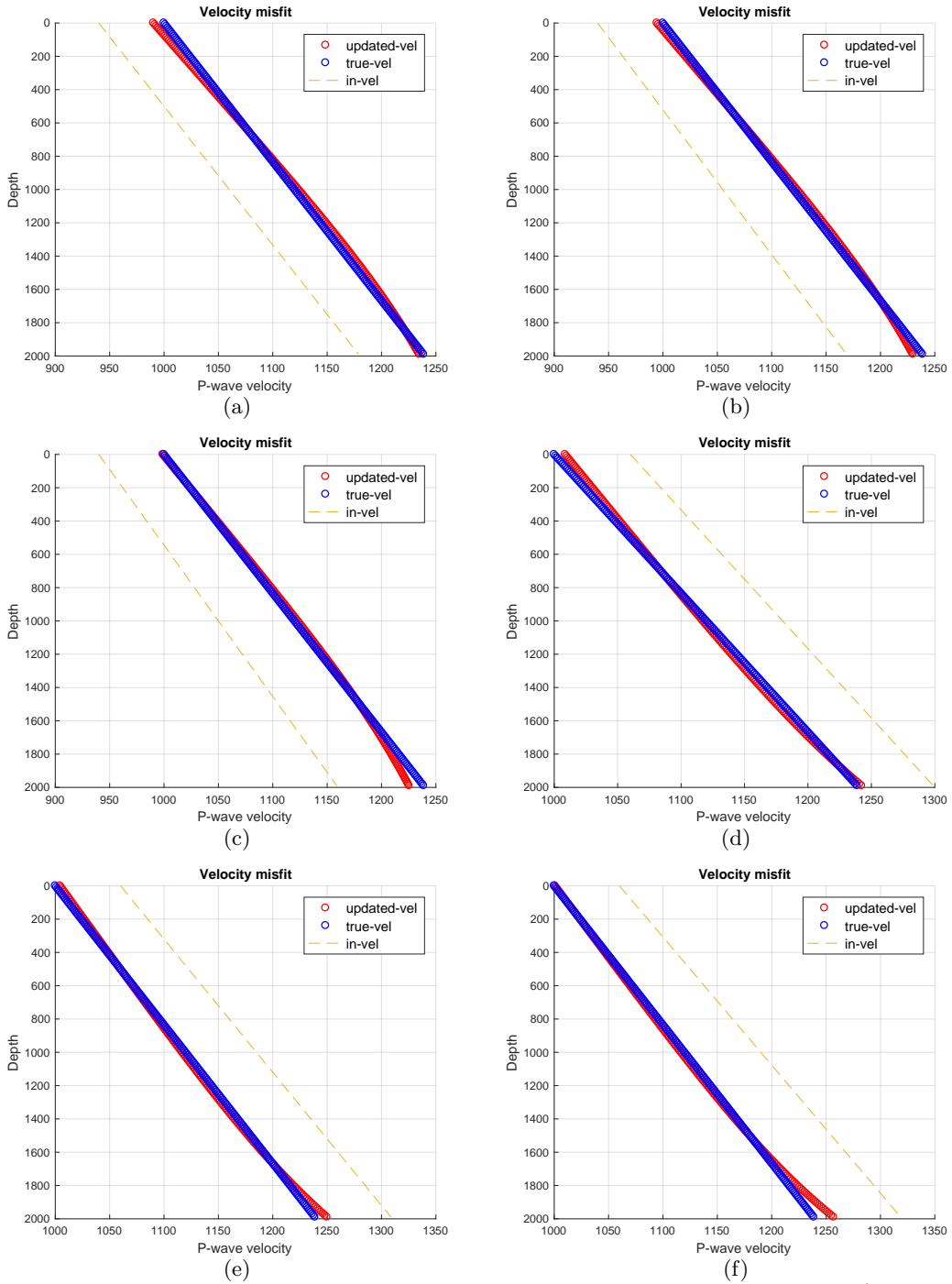


Figure 8: Velocity model for different velocity gradients,  $v_{in} = v_{true} \pm 60 (ms^{-1})$ .

## 4 1-D tomography : Application in real data

In this section, we apply the 1-D tomography and two-parameter inversion methods to a field data (??). In the two-parameter inversion, the traveltimes expression is used from Slawinski and Slawinski (1999). We develop the codes for both methods in Matlab and provide the source codes in the appendices A.1, A.2, and A.3.

In Table 3, we use the traveltimes data from Appendix ???. The total number of data points is 54, and the receivers are located up to the depth of 2650.20 m. In a real case study, the velocity results from 1-D traveltimes tomography can be in any order with depth. To get the linear inhomogeneity parameters, we use linear regression on the inverted velocity.

We also apply the real data on the  $ab$  model to calculate a global  $a$  and  $b$ . In Table 3, for the range of startup values, the two-parameter velocity inversion results do not change. The values of  $a$  and  $b$  are  $1247.07 \text{ ms}^{-1}$  and  $0.4384 \text{ s}^{-1}$ . However, the inversion results of the tomography are sensitive to the startup values. The low number of data points makes the inversion problem more sensitive to startup values.

The traveltimes convergence results are shown in Figure 9. The velocity misfits of the inverted velocity to the reference velocity are shown in Figure 10. Based on the synthetic experiments, we know that the inverted velocity reproduces the reference velocity with less error if the traveltimes convergence occurs faster. Therefore, we perform several tests with a range of startup values and show that tests 3 and 4 have the best startup values out of the six tests. Based on the results of experiments 3 and 4, we intuit that the inhomogeneity of the medium ranges from  $0.3960 \text{ s}^{-1}$  to  $0.4037 \text{ s}^{-1}$ . The inhomogeneity results can be improved by increasing the number of data points.

Test	$a_{in}$	$b_{in}$	$a_{inv}$	$b_{inv}$	$a_{tab}$	$b_{tab}$	$f(\mathbf{M})$	Figure
1	1225	0.40	1258.66	0.4373	1247.07	0.4384	52.01	9a,10b
2	1250	0.40	1271.63	0.4228	1247.07	0.4384	52.72	9b,10a
3	1285	0.40	1288.79	0.4037	1247.07	0.4384	51.55	9c,10c
4	1300	0.40	1295.85	0.3960	1247.07	0.4384	49.48	9d,10d
5	1315	0.40	1302.69	0.3885	1247.07	0.4384	53.79	9e,10e
6	1340	0.40	1313.67	0.3765	1247.07	0.4384	50.59	9f,10f

Table 3: Results of 1-D tomography and two-parameter method using real data (units of  $a$  and  $b$  are  $\text{ms}^{-1}$  and  $\text{s}^{-1}$ )

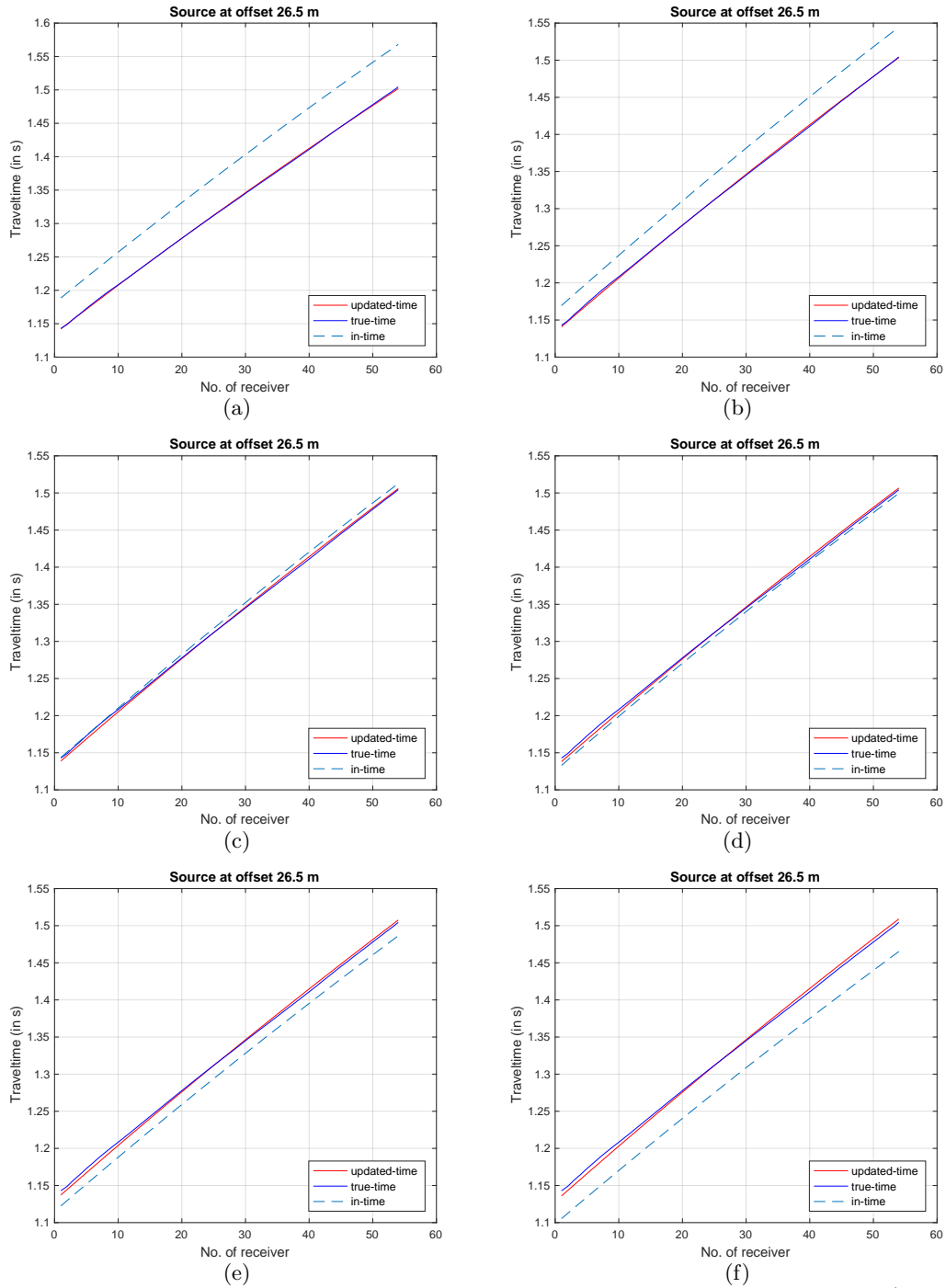


Figure 9: Traveltime inversion for different velocity gradients,  $v_{in} = v_{true} \pm 60 (ms^{-1})$ .

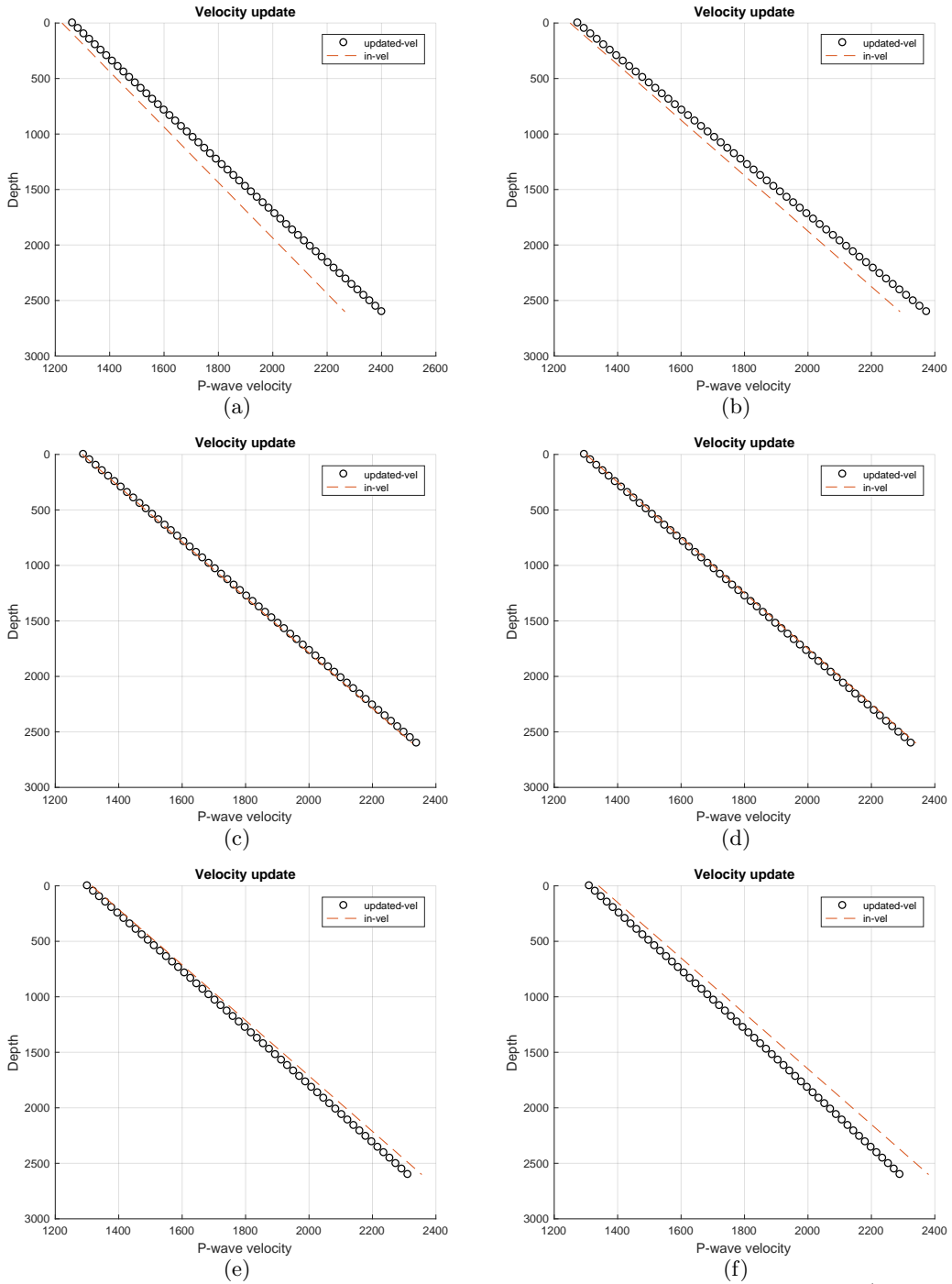


Figure 10: Velocity model for different velocity gradients,  $v_{in} = v_{true} \pm 60 (ms^{-1})$ .

## 5 Conclusion

The synthetic experiments show that the tomography method can reproduce the reference velocity with some misfits. The misfit gets higher when there is more noise, and fewer data points.

From the two-parameter method, we find that the inhomogeneity parameter,  $b$ , is higher in comparison to the 1-D tomography.

Since, from the traveltimes data, the 1-D tomography calculates  $m$  parameters and the  $ab$  method computes only two parameters to obtain velocity, therefore, we intuit that, for finding the local inhomogeneity of a segment, the 1-D tomography method is more reliable.

In practical seismology, the velocities are measured in the well log after a few hundred meters of depth from the surface. The VSP method can be used as a proxy to obtain the inhomogeneity parameters above the well log region.

For a common region of interest, we state that the study allows us to obtain linear inhomogeneity of a medium using two different seismic methods. To examine that statement, as a future project, we plan to do a comparison study by applying the developed methods on different sites.

## Acknowledgments

We acknowledge discussions with Michael A. Slawinski and proof reading of David R. Dalton. This research was performed in the context of The Geomechanics Project supported by Husky Energy. Also, this research was partially supported by the Natural Sciences and Engineering Research Council of Canada, grant 202259.

## References

- C-NLOPB (2019). Canada-Newfoundland & Labrador Offshore Petroleum Board website. <https://www.cnlopb.ca>.
- Červený, V. (2001). *Seismic ray theory*. Cambridge university press.
- Heath, M. T. (2002). *Scientific Computing*. The McGraw-Hill Companies, 2nd edition.
- Levenberg, K. (1944). A method for the solution of certain non-linear problems in least squares. *American Mathematical Society*, II(2).
- Marquardt, D. W. (1963). An algorithm for least-squares estimation of nonlinear parameters. *J. Soc. Indust. Appl. Math.*, II(2).
- Pujol, J. (2007). The solution of nonlinear inverse problems and the levenberg-marquardt method. *Geophysics*, 72(4).
- Pujol, J., Burrige, R., and Smithson, S. B. (1985). Velocity determination from offset vertical seismic profiling data. *Journal of Geophysical Research*, 90(B2):1871–1880.
- Slawinski, M. A. (2015). *Waves and rays in elastic continua*. World Scientific, 3rd edition.
- Slawinski, R. A. and Slawinski, M. A. (1999). On raytracing in constant velocity-gradient media: Calculus approach. *Canadian Journal of Exploration Geophysics*, 35(1/2):24–27.
- Zhdanov, M. S. (2002). *Geophysical inverse theory and regularization problems*. Elsevier.

# Appendix A

## A.1 1-D tomography : synthetic data

```
1 close all; clear all ;clc
2
3 %% Variables from travel time data
4 rec_depth = 1985:15:2000; % Creating data array for Geophones
5 offset_fict = 0:20:2000; % Creating data array for Sources
6                               % 201 sources at the surface with 20m apart from
7 N = length(rec_depth)*length(offset_fict);% Number of Layers (= Number of
   model parameters)
8 z_p = 0:(rec_depth(end)/N):rec_depth(end);
9 M = length(rec_depth); % Number of Geophone
10 S_N = length(offset_fict); % Number of sources
11
12 for i=1:S_N
13     for k=1:M
14         x_obs(k,i) = offset_fict(i);
15     end
16 end
17 %
18
19 %%%%%%%%%%% Similar_to_previous %%%%%%%%%%%
20 for i = 1:N
21     d_z_p(i) = z_p(i+1)-z_p(i); % layer thickness
22 end
23
24
25 for k = 1:M
26     for j = 1:N
27         H_n(k,j)=d_z_p(1);
28     end
29 end
30
31 for k = 1:M
32     for j = 1:N-1
33         H_n(k,j)=d_z_p(1);
34         if sum(d_z_p(1:(j))) <= rec_depth(k)
35             H(k,j)=d_z_p(j);
36             H(k,j+1)= rec_depth(k)-sum(d_z_p(1:(j)));
37         end
38     end
39 end
40
41
42 %% Variables for initial velocity and ray parameter
43 a = 1000;
44 b = .12;
45
46 %% From here complication starts
47 for j=1:N
```

```

48     v_o_true(j) = a+(b.*z_p(j));
49     v_o(j) = (a+20)+((b).*z_p(j));
50 end
51
52
53 v_true = v_o_true;
54 v_in = v_o;
55
56
57 %%%%%%%%%%%%%%%%%%%%%%%%%%%%%%%%%%%%%%%%%%%%%%%%%%%%%%%%%%%%%%%%%%%%%%%%%% Newton's Gradient %%%%%%%%%%%%%%%%%%%%%%%%%%%%%%%%%%%%%%%%%%%%%%%%%%%%%%%%%%%%%%%%%%%%%%%%%%
58 % Initial guess for theta_in to use in Newton method
59 for i=1:S_N
60     for k=1:M
61         theta_true(k,i) = atan(x_obs(k,i) ./ rec_depth(k));
62     end
63 end
64
65 % Initialize the iteration for Newton-Raphson method
66 for i=1:S_N
67     for k=1:M
68         dx_true(k,i) = 2500; % Initialize the iteration with higher values
69     end
70 end
71
72 myCoordList_true=[]; Ite_true = 0;
73 lim_dx_true = 1e-6;
74 while (abs(dx_true(:,end)) > lim_dx_true)
75
76     for i=1:S_N
77         for k=1:M
78             ray_p_o_i_true(k,i) = sin(theta_true(k,i)) ./ v_o_true(1);
79         end
80     end
81
82     for i=1:S_N
83         for k=1:M
84             for j = 1:N
85                 B_kji_i_true(k,j,i) = ray_p_o_i_true(k,i)*v_o_true(j);
86
87                 x_jki_true(j,k,i) = H(k,j) .* B_kji_i_true(k,j,i) ./ (1 -
                        B_kji_i_true(k,j,i).^2).^(.5);
88
89
90                 dx_prime_t1_true(j,k,i) = (H(k,j) .* v_o_true(j) .* cos(
                        theta_true(k,i))) ...
                        ./ (v_o_true(1) .* (1 - B_kji_i_true(k,j,i).^2).^(.5));
91
92
93                 dx_prime_t2_true(j,k,i) = (H(k,j) .* v_o_true(j) .* cos(
                        theta_true(k,i)) .* B_kji_i_true(k,j,i)) ...
                        ./ (v_o_true(1) .* (1 - B_kji_i_true(k,j,i).^2).^1.5);
94
95                 dx_true_all_prime(j,k,i) = dx_prime_t1_true(j,k,i)+

```

```

dx_prime_t2_true(j,k,i);
97     end
98   end
99 end
100
101 for i = 1:S_N
102   for k = 1:M
103     x_ki_true(k,i)=sum(x_jki_true(1:N,k,i)); % in m
104     dx_true_prime(k,i)= sum(dx_true_all_prime(1:N,k,i));
105   end
106 end
107 dx_true = abs(x_obs - x_ki_true);
108 theta_true = theta_true - (dx_true./dx_true_prime);
109 Ite_true = Ite_true+1;
110 myCoordList_true=[myCoordList_true; [Ite_true]];
111 end
112
113 for i=1:S_N
114   for k=1:M
115     ray_p_true(k,i) = sin(theta_true(k,i))./ v_o_true(1);
116   end
117 end
118
119 for i=1:S_N
120   for k=1:M
121     for j = 1:N
122       t_jki_true(j,k,i) = H(k,j)./(v_o_true(j).*(1-(ray_p_true(k,i)
123         .*v_o_true(j)).^2).^(.5)); % in s
124     end
125   end
126 end
127 for i = 1:S_N
128   for k = 1:M
129     t_ki_true(k,i)=sum(t_jki_true(1:N,k,i)); % in s
130   end
131 end
132
133 %%%%%%%%% Optimization Starts %%%%%%%%%
134
135 lambda = 1; misfit_fn = 10^4; Ite_m = 0; myCoordList_m=[];
136 myCoordList_t_ki = [];
137 while (misfit_fn >= 202)
138
139 %%%%%%%%%%%%%%%%%%%%%%%%%%%%% Newton-Raphson method %%%%%%%%%%%%%%%%%%%%%%%%%%%%%
140 % Initial guess for theta_in to use in Newton-Raphson method
141 for i=1:S_N
142   for k=1:M
143     theta_in(k,i) = atan(x_obs(k,i)./ rec_depth(k));
144   end
145 end
146 % Initialize the iteration for Newton method

```

```

147 myCoordList_in=[];Ite_in = 0;
148 for i=1:S_N
149     for k=1:M
150         dx_in(k,i) = 2500; % Initialize the iteration with higher values
151     end
152 end
153
154
155 myCoordList_in=[];Ite_in = 0;
156 lim_dx_in = 1e-6;
157 while (abs(dx_in(:,end)) > lim_dx_in)
158
159     for i=1:S_N
160         for k=1:M
161             ray_p_o_i_in(k,i) = sin(theta_in(k,i))./ v_o(1);
162         end
163     end
164
165     for i=1:S_N
166         for k=1:M
167             for j = 1:N
168                 B_kji_i_in(k,j,i) = ray_p_o_i_in(k,i)*v_o(j);
169
170                 x_jki_in(j,k,i) = H(k,j) .* B_kji_i_in(k,j,i) ./ (1 -
                    B_kji_i_in(k,j,i).^2).^(.5);
171
172
173                 dx_prime_t1_in(j,k,i) = (H(k,j) .* v_o(j) .* cos(theta_in(k,i)))
                    ...
                    ./ (v_o(1) .* (1 - B_kji_i_in(k,j,i).^2).^(.5));
174
175
176                 dx_prime_t2_in(j,k,i) = (H(k,j) .* v_o(j) .* cos(theta_in(k,i)) .*
                    B_kji_i_in(k,j,i)) ...
                    ./ (v_o(1) .* (1 - B_kji_i_in(k,j,i).^2).^1.5);
177
178
179                 dx_in_all_prime(j,k,i) = dx_prime_t1_in(j,k,i)+dx_prime_t2_in(
                    j,k,i);
180             end
181         end
182     end
183
184     for i = 1:S_N
185         for k = 1:M
186             x_ki_in(k,i)=sum(x_jki_in(1:N,k,i)); % in m
187             dx_in_prime(k,i)= sum(dx_in_all_prime(1:N,k,i));
188         end
189     end
190 dx_in = abs(x_obs - x_ki_in);
191 theta_in = theta_in - (dx_in./dx_in_prime);
192 Ite_in = Ite_in+1;
193 myCoordList_true=[myCoordList_in; [Ite_in]];
194 end

```

```

195
196 for i=1:S_N
197     for k=1:M
198         ray_p_in(k,i) = sin(theta_in(k,i))./ v_o(1);
199     end
200 end
201
202 for i=1:S_N
203     for k=1:M
204         for j = 1:N
205             B_kji(k,j,i) = ray_p_in(k,i).*v_o(j);
206             t_jki_in(j,k,i) = H(k,j)./(v_o(j).*(1-(B_kji(k,j,i)).^2).^(.5)
                ); % in s
207         end
208     end
209 end
210
211 for i = 1:S_N
212     for k = 1:M
213         t_ki_in(k,i)=sum(t_jki_in(1:N,k,i)); % in s
214     end
215 end
216
217
218 %Calculation of the derivatives from initial estimates
219 for i=1:S_N
220     for k=1:M
221         for j = 1:N
222             ddvj_tk(k,j,i) = -H_n(k,j)./(v_o(j).^2.*(1-B_kji(k,j,i).^2)
                .^(.5))...
223             + (ray_p_in(k,i).^2.*H_n(k,j))./(1-B_kji(k,j,i).^2).^1.5)
                ;
224         end
225     end
226 end
227
228
229 %%%%%%%%%%%%%%%%%%%%%%%%%%%%%%%%%%%%%%%%%% Adding_Noise %%%%%%%%%%%%%%%%%%%%%%%%%%%%%%%%%%%%%%%%%%
230 t = t_ki_in(:);
231 t_true = t_ki_true(:);
232 noiseSigma = 0.01 * t_true; % standard deviation = noiseSigma
233 noise = noiseSigma .* randn(length(t_true),1); % considering mean = 0
234 noisySignal = t_true + noise;
235 Y_c = noisySignal;
236 dt = (Y_c - t);
237 dt = reshape(dt,[M,S_N]);
238 noise = reshape(noise,[M,S_N]);
239 Y_c = reshape(Y_c,[M,S_N]);
240 %%%%%%%%%%%%%%%%%%%%%%%%%%%%%%%%%%%%%%%%%% Adding_Noise %%%%%%%%%%%%%%%%%%%%%%%%%%%%%%%%%%%%%%%%%%
241
242 for i=1:S_N
243     for k=1:M

```

```

244         for j = 1:N
245             term_A1(k,j,i) = ddvj_tk(k,j,i);
246         end
247     end
248 end
249
250 term_A = [term_A1];
251 %%
252 %
%%%%%%%%%%%%%%%%%%%%%%%%%%%%%%%%%%%%%%%%%%%%%%%%%%%%%%%%%%%%%%%%%%%%%%%%%%
253 %%%%%%%%%%%%%%%%%%%%%%%%%%%%%%%%%%%%%%%%%%%%%%%%%%%%%%%%%%%%%%%%%%%%%%%%%%% Conversion to vectors and matrix
%%%%%%%%%%%%%%%%%%%%%%%%%%%%%%%%%%%%%%%%%%%%%%%%%%%%%%%%%%%%%%%%%%%%%%%%%%
254
255 C = dt(:);
256
257 A_c_terms = [];
258 for ll = 1:size(term_A,3)
259     A_c_terms = cat(1,A_c_terms,term_A(:,:,ll));
260 end
261 A = A_c_terms;
262
263 A_T_A = transpose(A)*A;
264 A_T_C = transpose(A)*C;
265
266 for i = 1:(N)
267     for j = 1:(N)
268         if i==j
269             s_ij(i,j)=1./sqrt(A_T_A(i,j));
270         elseif i ~= j
271             s_ij(i,j)=0;
272         end
273     end
274 end
275 S = s_ij;
276 A_T_A_ast = S.'*A_T_A*S;
277 A_T_C_ast = S.'*A_T_C;
278
279 I = eye(N,N);
280 lambda = I*1000;
281
282 inv_t_ast = A_T_A_ast+lambda;
283 X_ast = inv(inv_t_ast)*A_T_C_ast;
284 X = S.'* X_ast;
285
286
287 dt_up = dt(:);
288 misfit_fn = (sum((dt_up(:)./noise(:)).^2));
289
290 dv = X.';
291 v_o = v_o + dv;
292 v_f = v_o;

```

```

293 lambda = lambda * 0.1;
294 Ite_m = Ite_m+1;
295 myCoordList_m=[myCoordList_m; [Ite_m, misfit_fn]];
296 myCoordList_t_ki=[myCoordList_t_ki; [t_ki_in]];
297 %%%%%%%%%%%%%%%%%%%%%%%%%%%%%%%%%%%%%%%%%%%%%%%%%%%%%%%%%%%%%%%%%%%%%%%%%end%%%%%%%%%%%%%%%%%%%%%%%%%%%%%%%%%%%%%%%%%%%%%%%%%%%%%%%%%%%%%%%%%%%%%%%%
298 end
299
300 %%%%%%%%%%%%%%%%%%%%%%%%%%%%%%%%%%%%%%%%%%%%%%%%%%%%%%%%%%%%%%%%%%%%%%%%%end%%%%%%%%%%%%%%%%%%%%%%%%%%%%%%%%%%%%%%%%%%%%%%%%%%%%%%%%%%%%%%%%%%%%%%%%
301 figure(1) % Traveltime plot
302 %%%%%%%%%%%%%%%%%%%%%%%%%%%%%%%%%%%%%%%%%%%%%%%%%%%%%%%%%%%%%%%%%%%%%%%%%
303 subplot(2,1,1)
304 time_k1_in = myCoordList_t_ki(1,:);
305 time_k1_true = t_ki_true(1,:);
306 time_k1_f = t_ki_in(1,:);
307 NT = Y_c(1,:); %Noisy Traveltime
308 err = noise(1,:);
309 err = std(err).*ones(size(err));
310
311 indx = 1:1:length(NT);
312 scatter(indx,NT);
313 hold on;
314 errorbar(indx, NT, err, 'LineStyle','none');
315 hold on;
316
317 plot(time_k1_f, 'r')
318 hold on
319
320 plot(time_k1_true, 'b')
321 hold on
322
323 plot(time_k1_in, '—')
324 legend({'noisy data','errorbar','updated-time','true-time','in-time'},'
Location','southeast','FontSize',8)
325 xlabel('No. of source','FontSize',12)
326 ylabel('Traveltime (in s)','FontSize',12)
327 title('Traveltime misfit_fn at R_{1}','FontSize',10)
328 grid on
329
330
331 % When more than one receiver
332 subplot(2,1,2)
333 time_k1_in = myCoordList_t_ki(2,:);
334 time_k1_true = t_ki_true(2,:);
335 time_k1_f = t_ki_in(2,:);
336 NT = Y_c(2,:); %Noisy Traveltime
337 err = noise(2,:);
338 err = std(err).*ones(size(err));
339
340 indx = 1:1:length(NT);
341 scatter(indx,NT);
342 hold on;
343 errorbar(indx, NT, err, 'LineStyle','none');

```

```

344 hold on;
345
346 plot(time_k1_f, 'r')
347 hold on
348
349 plot(time_k1_true, 'b')
350 hold on
351
352 plot(time_k1_in, '—')
353 legend({'noisy data', 'errorbar', 'updated-time', 'true-time', 'in-time'}, '
      Location', 'southeast', 'FontSize', 8)
354 xlabel('No. of source', 'FontSize', 12)
355 ylabel('Traveltime (in s)', 'FontSize', 12)
356 title('Traveltime misfit_fn at R_{2}', 'FontSize', 10)
357 grid on
358
359
360
361 %%%%%%%%%%%%%%%%%%%%%%%%%%%%%%%%%%%%%%%%%%%%%%%%%%%%%%%%%%%%%%%%%%%%%%%%%%
362 figure(2) % Velocity plot
363 %%%%%%%%%%%%%%%%%%%%%%%%%%%%%%%%%%%%%%%%%%%%%%%%%%%%%%%%%%%%%%%%%%%%%%%%%%
364
365
366 z_p_plot = z_p(1:end-1);
367 scatter(v_f, z_p_plot, 'r')
368 hold on
369 scatter(v_true, z_p_plot, 'b')
370 hold on
371 plot(v_in, z_p_plot, '—')
372 legend({'updated-vel', 'true-vel', 'in-vel'}, 'Location', 'northeast', '
      FontSize', 12)
373 set(gca, 'Ydir', 'reverse')
374 xlabel('P-wave velocity', 'FontSize', 12)
375 ylabel('Depth', 'FontSize', 12)
376 title('Velocity misfit_fn', 'FontSize', 12)
377 grid on

```

## A.2 1-D tomography : real data

```
1 close all; clear all ;clc
2 %% Data upload
3 [num,txt ,raw] = xlsread('mizzen_o_16_cs.xlsx'); % Checkshot data
4 vert_depth = num(:,2);
5 vert_depth = rmmissing(vert_depth)-5; % True vertical depth from source)
6 travelttime = num(:,3);
7 travelttime = rmmissing(travelttime); % Measured travelttime from source to
   receivers
8 travelttime = travelttime(1:54);
9 offset = 26.5; % Source offset 26.5 m
10 sigma = .0003; % from time picking
11
12 %% Variables from travel time data
13 rec_depth = vert_depth(1:54).';
14 z_p = 0:(rec_depth(end)/54):rec_depth(end);
15 N = length(z_p)-1;
16 M = length(rec_depth); % Number of Geophone
17 S_N = length(offset); % Number of sources
18
19
20 for i=1:S_N
21     for k=1:M
22         x_obs(k,i) = offset(i);
23     end
24 end
25 %
26
27 %%%%%%%%%%% Similar_to_previous %%%%%%%%%%%
28 for i = 1:N
29     d_z_p(i)= z_p(i+1)-z_p(i); % layer thickness
30 end
31
32
33 % Not working this H?
34 for k = 1:M
35     for j = 1:N
36         H_n(k,j)=d_z_p(1);
37     end
38 end
39
40 for k = 1:M
41     for j = 1:N-1
42         H_n(k,j)=d_z_p(1);
43         if sum(d_z_p(1:(j))) <= rec_depth(k)
44             H(k,j)=d_z_p(j);
45             H(k,j+1)= rec_depth(k)-sum(d_z_p(1:(j)));
46         end
47     end
48 end
49
```

```

50
51 %% Variables for initial velocity and ray parameter
52 a_in = 1250;
53 b_in = 0.40;
54
55 %% Initial Velocity
56 for j=1:N
57     v_o(j) = a_in+(b_in.*z_p(j));
58 end
59 v_in = v_o;
60
61
62
63 %%%%%%%%% Optimization Starts %%%%%%%%%
64 %%%%%%%%% Initialize Levenberg-Marquardt Method %%%%%%%%%
65 lambda = 1e3; misfit_fn = 10^4; Ite_m = 0; myCoordList_m=[];
66 myCoordList_t_ki = [];
67 while (misfit_fn >= 54)
68
69 %%%%%%%%%%%%%%% Newton's Gradient %%%%%%%%%%%%%%%
70 % Initial guess for theta_in to use in Newton method
71 for i=1:S_N
72     for k=1:M
73         theta_in(k,i) = atan(x_obs(k,i) ./ rec_depth(k));
74     end
75 end
76 % Initialize the iteration for Newton method
77 myCoordList_in=[]; Ite_in = 0;
78 for i=1:S_N
79     for k=1:M
80         dx_in(k,i) = 2500;
81     end
82 end
83
84
85 myCoordList_in=[]; Ite_in = 0;
86 lim_dx_in = 1e-10;
87 while (abs(dx_in(:,end)) > lim_dx_in)
88
89 for i=1:S_N
90     for k=1:M
91         ray_p_o_i_in(k,i) = sin(theta_in(k,i)) ./ v_o(1);
92     end
93 end
94
95 for i=1:S_N
96     for k=1:M
97         for j = 1:N
98             B_kji_i_in(k,j,i) = ray_p_o_i_in(k,i)*v_o(j);
99
100             x_jki_in(j,k,i) = H(k,j) .* B_kji_i_in(k,j,i) ./ (1 -
                B_kji_i_in(k,j,i).^2).^(.5);

```

```

101
102
103     dx_prime_t1_in(j,k,i) = (H(k,j) .* v_o(j) .* cos(theta_in(k,i)))
        ...
104     ./ (v_o(1) .* (1 - B_kji_in(k,j,i) .^ 2) .^ (.5));
105
106     dx_prime_t2_in(j,k,i) = (H(k,j) .* v_o(j) .* cos(theta_in(k,i)) .*
        B_kji_in(k,j,i)) ...
107     ./ (v_o(1) .* (1 - B_kji_in(k,j,i) .^ 2) .^ (1.5));
108
109     dx_in_all_prime(j,k,i) = dx_prime_t1_in(j,k,i) + dx_prime_t2_in(
        j,k,i);
110     end
111 end
112 end
113
114 for i = 1:S_N
115     for k = 1:M
116         x_ki_in(k,i) = sum(x_jki_in(1:N,k,i)); % in m
117         dx_in_prime(k,i) = sum(dx_in_all_prime(1:N,k,i));
118     end
119 end
120 dx_in = abs(x_obs - x_ki_in);
121 theta_in = theta_in - (dx_in ./ dx_in_prime);
122 Ite_in = Ite_in + 1;
123 myCoordList_true = [myCoordList_in; [Ite_in]];
124 end
125
126 for i = 1:S_N
127     for k = 1:M
128         ray_p_in(k,i) = sin(theta_in(k,i)) ./ v_o(1);
129     end
130 end
131
132 for i = 1:S_N
133     for k = 1:M
134         for j = 1:N
135             B_kji(k,j,i) = ray_p_in(k,i) .* v_o(j);
136             t_jki_in(j,k,i) = H(k,j) ./ (v_o(j) .* (1 - (B_kji(k,j,i) .^ 2) .^ (.5)
                )); % in s
137         end
138     end
139 end
140
141 for i = 1:S_N
142     for k = 1:M
143         t_ki_in(k,i) = sum(t_jki_in(1:N,k,i)); % in s
144     end
145 end
146
147
148 %Calculation of the derivatives from initial estimates

```

```

149 for i=1:S_N
150     for k=1:M
151         for j = 1:N
152             ddvj_tk(k,j,i) = -H_n(k,j) ./ (v_o(j).^2.*(1-B_kji(k,j,i).^2)
153                 .^(.5)) ...
154                 + (ray_p_in(k,i).^2.*H_n(k,j))./(1-B_kji(k,j,i).^2).^(1.5)
155                 ;
156         end
157     end
158 end
159 %%%%%%%%%%%%%%%%%%%%%%%%%%%%%%%%%%%%%%%%% Adding_Noise %%%%%%%%%%%%%%%%%%%%%%%%%%%%%%%%%%%%%%%%%
160 t = t_ki_in(:);
161 t_true = travelttime(:);
162 dt = (t_true - t);
163 dt = reshape(dt,[M,S_N]);
164 t_true = reshape(t_true,[M,S_N]);
165 %%%%%%%%%%%%%%%%%%%%%%%%%%%%%%%%%%%%%%%%% Adding_Noise %%%%%%%%%%%%%%%%%%%%%%%%%%%%%%%%%%%%%%%%%
166
167 for i=1:S_N
168     for k=1:M
169         for j = 1:N
170             term_A1(k,j,i) = ddvj_tk(k,j,i);
171         end
172     end
173 end
174
175 term_A = [term_A1];
176 %%
177 %%%%%%%%%%%%%%%%%%%%%%%%%%%%%%%%%%%%%%%%% Conversion to vectors and matrix %%%%%%%%%%%%%%%%%%%%%%%%%%%%%%%%%%%%%%%%%
178
179 C = dt(:);
180
181 A_c_terms = [];
182 for ll = 1:size(term_A,3)
183     A_c_terms = cat(1,A_c_terms,term_A(:,:,ll));
184 end
185 A = A_c_terms;
186
187 A_T_A = transpose(A)*A;
188 A_T_C = transpose(A)*C;
189
190 for i = 1:(N)
191     for j = 1:(N)
192         if i==j
193             s_ij(i,j)=1./sqrt(A_T_A(i,j));
194         elseif i ~= j
195             s_ij(i,j)=0;
196         end
197     end

```

```

198 end
199 S = s_ij;
200 A_T_A_ast = S.'*A_T_A*S;
201 A_T_C_ast = S.'*A_T_C;
202
203 I = eye(N,N);
204 lambda = I*1000;
205
206 inv_t_ast = A_T_A_ast+lambda;
207 X_ast = inv(inv_t_ast)*A_T_C_ast;
208 X = S.'* X_ast;
209
210
211 dt_up = dt(:);
212 misfit_fn = sum(dt_up(:)./sigma).^2;
213
214 dv = X.>';
215 v_o = v_o + dv;
216 v_f = v_o;
217 lambda = lambda * 0.1;
218 Ite_m = Ite_m+1;
219 myCoordList_m=[myCoordList_m; [Ite_m, misfit_fn]];
220 myCoordList_t_ki=[myCoordList_t_ki; [t_ki_in]];
221 end
222
223 %%%%%%%%%%%%%%%%%%%%%%%%%%%%%%%%%%%%%%%%%%%%%%%%%%%%%%%%%%%%%%%%%%%%%%%%%
224 figure(1)
225 %%%%%%%%%%%%%%%%%%%%%%%%%%%%%%%%%%%%%%%%%%%%%%%%%%%%%%%%%%%%%%%%%%%%%%%%%
226 time_k1_in = myCoordList_t_ki(1:54,1);
227 time_k1_true = t_true;
228 time_k1_f = t_ki_in;
229 time_k1_f = myCoordList_t_ki((end-53):end,1);
230
231 plot(time_k1_f, 'r')
232 hold on
233 plot(time_k1_true, 'b')
234 hold on
235 plot(time_k1_in, '—')
236 legend({'updated-time', 'true-time', 'in-time'}, 'Location', 'southeast', '
FontSize', 10)
237 xlabel('No. of receiver', 'FontSize', 12)
238 ylabel('Traveltime (in s)', 'FontSize', 12)
239 title('Source at offset 26.5 m', 'FontSize', 12)
240 grid on
241
242 z_p_plot = z_p(1:end-1);
243 p_n = polyfit(z_p_plot, v_f, 1);
244 yfit = polyval(p_n, z_p_plot);
245 p_nn = polyfit(z_p_plot(39:end), v_f(39:end), 1);
246 yfitn = polyval(p_nn, z_p_plot(39:end));
247
248

```

```

249 %%%%%%%%%%%%%%%%%%%%%%%%%%%%%%%%%%%%%%%%%%%%%%%%%%%%%%%%%%%%%%%%%%%%%%%%%%
250 figure(2)
251 %%%%%%%%%%%%%%%%%%%%%%%%%%%%%%%%%%%%%%%%%%%%%%%%%%%%%%%%%%%%%%%%%%%%%%%%%%
252 scatter(v_f , z_p_plot , 'k')
253 hold on
254 plot(v_in , z_p_plot , '--')
255 legend('updated-vel' , 'in-vel')
256 set(gca , 'Ydir' , 'reverse')
257 xlabel('P-wave velocity' , 'FontSize' , 12)
258 ylabel('Depth' , 'FontSize' , 12)
259 title('Velocity update' , 'FontSize' , 12)
260 grid on
261
262 upd = [a_in b_in p_n(1,2) p_n(1,1) p_nn(1,2) p_nn(1,1) misfit_fn]
263
264
265 rec_depth_t = rec_depth.';
266 ind_t = 1:length(rec_depth_t);
267 ind_t = ind_t.';
268
269 upd_t = [ind_t rec_depth_t travelttime];

```

### A.3 *ab* model inversion : real data

```
1 close all; clear all ;clc
2 [num,txt ,raw] = xlsread('mizzen_o_16_cs.xlsx'); % Checkshot data
3 vert_depth = num(:,2);
4 vert_depth = rmmissing(vert_depth)-5; % True vertical depth from source
   (-5 because MSL-SP=5m)
5 travelttime = num(:,3);
6 travelttime = rmmissing(travelttime); % Measured travelttime from source to
   receiver
7 travelttime = travelttime(1:54);
8 offset = 26.5; % Source offset 26.5 m
9
10
11 %% Variables from travel time data
12 rec_depth = vert_depth(1:54);
13 d_p =length(rec_depth);
14
15
16
17 Depth_of_layer = 0; % in m
18 Depth_of_receiver = rec_depth; % in m
19 z = Depth_of_receiver - Depth_of_layer;
20 x_o = offset;
21 t_d = travelttime(1:d_p,1);
22 a_in = 1285;
23 b_in = .40;
24
25 lb=[eps eps];
26 ub=[inf inf];
27 x0=[a_in b_in];
28
29
30 fun = @(X)fn_ab(X(1),X(2), z, x_o, t_d);
31 x = lsqnonlin(fun,x0,lb,ub)
32
33 a_p = x(1);
34 b_p = x(2);
35
36 t_test = fn_ab(a_p,b_p, z, x_o, t_d);
37 mis_fit = sqrt(t_test.^2);
38 t_mean = mean(t_test)
39
40
41 function fun=fn_ab(a, b, z, x, t_d)
42 p_b_1 = (b.^2.*x.^2) + a.^2 + (a+b.*z).^2;
43 p_b_2 = 2.*a.*(a+b.*z);
44 p = (2.*b.*x)./sqrt(p_b_1.^2-p_b_2.^2);
45
46 term_3 = (a + (b.*z))./a;
47 term_4 = sqrt(1-(a.^2).*(p.^2));
48 term_5 = sqrt(1-((term_3.*a).^2).*(p.^2));
```

```
49
50 t_time = (1./b).*log( (term_3).*((1+term_4)./(1+term_5)));
51
52 fun = abs(t_time - t_d);
53 end
```